

## A NEURAL NETWORK APPROACH TO PREDICT THE IONOSPHERIC SCINTILLATION WBMOD MODEL VARIABLES

<sup>1</sup>C. Molina, <sup>1</sup>B.E. Boudriki Semlali, <sup>1</sup>H. Park, <sup>1,2</sup>A. Camps

<sup>1</sup>CommSensLab-UPC– Dep. of Signal Theory and Communications and IIEC/CTE-UPC, Universitat Politècnica de Catalunya - Campus Nord, E-08034 Barcelona

<sup>3</sup>ASPIRE Visiting International Professor at UAE University, CoE, PO Box 15551, Al Ain, UAE

### ABSTRACT

The ionospheric scintillation can be explained as the fluctuations in the phase and intensity of electromagnetic rays after crossing the ionosphere. Rino's theory was proposed in 1979 to quantify this scintillation, and subsequent models appeared to predict its characteristics. One of them is the WideBand ionospheric scintillation Model (WBMOD) from 1984. This study aims to provide a neural network that emulates the behavior of WBMOD model, by learning from phase and intensity scintillation data gathered from several ESA projects. By using the Rino's power-law phase-screen ionospheric scintillation theory, the values of the height-integrated irregularities strength ( $C_k L$ ) and the slope of its PSD ( $q$ ) can be obtained from the physically measured  $S_4$  and  $\sigma_\phi$ . So, using this data, two neural networks are presented which obtains results that fit well with the WBMOD expected values.

**Index Terms**— WBMOD, Ionospheric Scintillation, Neural-network

### 1. INTRODUCTION

The WideBand ionospheric scintillation Model (WBMOD) [1, 2] is a climatological model that computes ionospheric scintillation on radio-wave propagation for frequencies higher than 100 MHz. The model provides climatological data of the ionospheric F-layer, using a power-law, phase-screen propagation model [3]. The model outputs include the axial ratio for the shape of the irregularities (a, b), the irregularities' strength ( $C_k L$ ), its PDS slope ( $q$ ), and the in-situ drift velocities, given a certain number of inputs: the geographic location (lat, lon), the Magnetic Local Time (MLT), the day of the year (DoY), the planetary index (Kp), the smoothed Zurich sunspot number (R12), and a percentile (PERC).

The UPC has participated in several recent projects (SCIONAV [4], CLIMIONO [5]) for the European Space Agency (ESA), in cooperation with the French Aerospace Lab ONERA and the company Research and Development in Aerospace GmbH in Switzerland (RDA). Particularly, CLIMIONO is a project that uses experimental ionospheric

observations in the last years to assess the performance of climatological models focusing on ionospheric scintillation.

The purpose of this work is to use the phase and intensity scintillation data from these projects to get the corresponding WBMOD variables, in particular  $q$  and  $C_k L$ , and then train a neural network (NN) to emulate the WBMOD model, yielding in a faster and freely available approximation of the model.

### 2. DATA SOURCES AND METHODOLOGY

The first step is to know which data will be needed to properly fit the NN. First, we have the scintillation data in the form of phase ( $\sigma_\phi$ ) and intensity ( $S_4$ ), that are geolocated (lat, lon), and time tagged (UTC). Using the equations from the phase-screen model for ionospheric scintillation from Rino (1979) [3], we can obtain the parameters used in the WBMOD. In this model, the phase scintillation is computed as follows. The temporal power spectrum of phase is given by the Fourier integral:

$$\varphi(f) = \int_{-\infty}^{+\infty} R_{\delta\phi}(v_{\text{eff}}\delta t) \cos(2\pi i f \delta t) d\delta t \quad (1)$$

which can be evaluated as:

$$\varphi(f) = \frac{T}{(f_0^2 + f^2)^{p/2}} \quad (2)$$

where  $p = 2\nu$ ,  $f_0 = \frac{v_{\text{eff}} q_0}{2\pi} = v_{\text{eff}} l_0$ , and

$$T = r_e^2 \lambda^2 (L \sec \theta) G C_k \frac{\sqrt{\pi} \Gamma(\nu)}{(2\pi)^{2\nu+1} \Gamma(\nu + 1/2)} v_{\text{eff}}^{2\nu-1} \quad (3)$$

By integrating (2) over all frequencies we get the phase variance:

$$\langle \delta\Phi^2 \rangle = r_e^2 \lambda^2 G C_k L \sec \theta \frac{q_0^{-2\nu+1} \Gamma(\nu - 1/2)}{4\pi \Gamma(\nu + 1/2)} \quad (4)$$

where  $r_e$  is the classical electron radius,  $\lambda$  is the wave length,  $G$  is the phase enhancement factor, defined in eqn 10 of Rino

(1979),  $C_k$  is the strength of turbulence defined in eqn 7 of Rino (1979),  $L$  is the layer thickness,  $\theta$  is the propagation (nadir) angle at the ionospheric pierce-point,  $q_0$  is the outer-scale cutoff wave number, and  $\nu$  is the spectral index parameter, related to  $q$  with  $q = 2\nu - 1$ . Note that  $\Gamma$  is the gamma function.

Regarding the intensity scintillation ( $S_4$ ), eqn 4 from Carrano (2019), taken from Rino (1979), relates this index to the height-integrated irregularity strength ( $C_k L$ ):

$$S_{4w}^2 = \left\{ r_e^2 \lambda^2 \sec \theta \left( \frac{2\pi}{1000} \right)^{2\nu+1} C_k L \right\} \rho_F^{2\nu-1} F_S(\nu) \mathcal{P}(\nu) \quad (5)$$

The sub-index  $w$  in  $S_{4w}$  indicates that this only accounts for the weak scatter phenomena. To include the multiple scatter effects which produce a strong scintillation, this formula should be corrected by the empirical expression (Fremouw & Secan, 1984) [6]:

$$S_4^2 \approx 1 - \exp(-S_{4w}^2). \quad (6)$$

In our study, using the measurements of  $S_4$  it is possible to get the  $S_{4w}$  value, and inverting eqn (5), obtain the  $C_k L$ . Additionally, from eqn (4) it can be obtained the value of  $q$ .

As the source data is provided geolocated and time-tagged, it is possible to retrieve the geomagnetic and space-weather parameters of each measurement, which are the magnetic local time (MLT), the planetary index ( $K_p$ ), and the smoothed sunspots number (R12), needed to match with the WBMOD model input parameters.

The variables that are fitted with the proposed neural networks are the  $C_k L$ , which exhibits dependence on all the variables mentioned (lat, lon, MLT,  $K_p$ , DoY, and R12), and the slope of the in-situ irregularities PSD ( $q$ ), which is only geographically dependent. Additionally, as both variables,  $C_k L$  and  $q$  have a more natural representation on the geomagnetic coordinate system, these inputs from the measurements have been transformed into these coordinates (glat, glon).

Moreover, variables like the longitude or the magnetic local time has a cyclic behavior. Particularly, in the case of the longitude, the values at  $-180^\circ$  must be the same as in  $+180^\circ$ , and for the local time it should also match the values at 0 and 24 h. If the fit is done without taking into account this constraint could get to discontinuities in the output value computed by the NN. To avoid that, a "circular" transformation have been applied to the input data before injecting it into the training. For the geomagnetic longitude it was converted to the following two inputs:

$$\text{glon}_s = \sin \left( \frac{\pi \text{glon}}{180} \right) \quad (7)$$

$$\text{glon}_c = \cos \left( \frac{\pi \text{glon}}{180} \right) \quad (8)$$

For MLT, only applicable for the  $C_k L$  training, it was done similarly with:

$$\text{MLT}_s = \sin \left( \frac{\pi \text{MLT}}{12} \right) \quad (9)$$

$$\text{MLT}_c = \cos \left( \frac{\pi \text{MLT}}{12} \right) \quad (10)$$

This way, after transforming back to the normal coordinates, it is ensured the continuity and smoothness of the neural network solution.

### 3. RESULTS

The results for the two neural networks designed for  $q$ , and  $C_k L$ , respectively, are presented in this section. For the  $q$  NN, after several iterations in the process of tuning the number of neurons, internal layers, neuron transfer functions, and learning algorithm, a reasonable good fit was obtained using a 4-hidden-layers fully-connected NN with two inputs (glat, glon) and 3, 6, 20, and 20 neurons per hidden layer respectively. The mean-squared error performance obtained is  $1.24 \cdot 10^{-6}$ , which compared to the average value  $\langle q \rangle = 1.6$ , means a  $7.7 \cdot 10^{-5}\%$ . The output value of  $q$  using this NN is shown in Fig. 1.

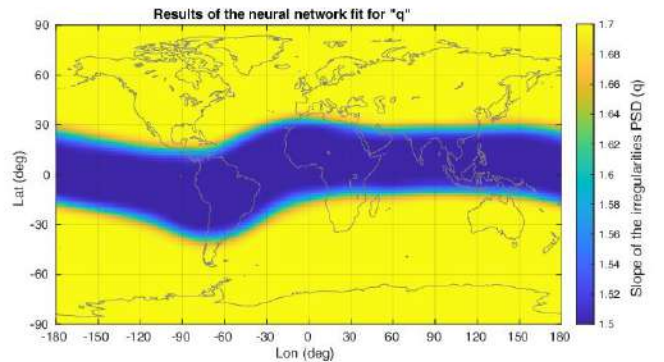


Fig. 1. Output of the NN for  $q$ .

The network for  $C_k L$  should be more complex as it depends on more input variables than the  $q$ . Apart from that, the difference between low and high values of the  $C_k L$  is too high for the network to converge, even after the normalization of the values done before the training of the data. To avoid this problem, a logarithmic transformation have been applied to the  $C_k L$  values before injecting into the training algorithm. This helps to reduce the dynamical range of the data and distribute the values more evenly.

After this pre-processing and several iterations in the search for a suitable network architecture, it was obtained a good result for a 5-hidden-layers fully-connected NN in which there were 11, 16, 40, 40, and 20 neurons per hidden

layer, 9 inputs, and 1 output. The neural network was trained with about 980 000 samples, and after 1 000 iterations, the NN converged and got a mean-squared error performance of 0.0056, which means around a  $(0.018 \pm 0.0025)\%$  error on the  $\log_{10}(C_k L)$ .

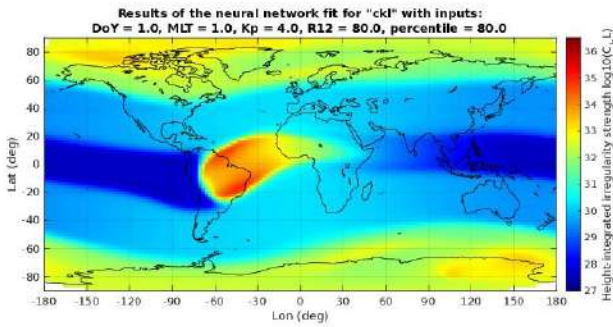


Fig. 2. Results of the NN for  $\log_{10}(C_k L)$ .

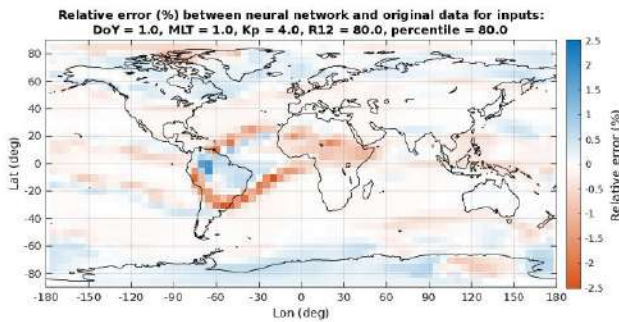


Fig. 3. Relative error  $\mathcal{E}$  (%) between the NN output and the WBMOD model outputs for  $C_k L$  in the same conditions as Fig. 2.

As observed in Fig. 2, the neural network is performing very well and reproducing almost every feature in the shape of  $C_k L$  from the model, as it can be checked by the relative error plot in Fig. 3. The relative error  $\mathcal{E}$  between the network outputs and the model outputs is computed as  $\mathcal{E} = 100 \frac{NN - WBMOD}{WBMOD}$ . In this scenario, the maximum deviation from the WBMOD model is around 2.5%, indicated in the color scale. This good behavior is mostly maintained when sweeping to other values of the MLT (0–24 h), Kp (1–9), R12 (0–200), and DoY (0–365). For very high values of the solar activity, represented by R12 above 160, the errors start to diverge from the model, producing errors of about 4% to 6%.

All the data pre-processing and neural network training has been performed with MATLAB and its Deep-Learning Toolbox. In both cases the learning method employed to train the network was the Levenberg-Marquardt retropropagation, and the transfer function of all neurons was the hyperbolic tangent sigmoid function (`tansig` in MATLAB).

## 4. CONCLUSIONS

In this study, the parameters needed to model the ionospheric scintillation indices ( $S_4$  and  $\sigma_\phi$ ) have been obtained from the Rino’s power-law phase screen parameters  $q$ , and  $C_k L$ , by using an approximation of the WBMOD model generated with a neural network. These neural networks have been trained with data obtained from some ESA projects in cooperation with the UPC CommSensLab, and it arrived to two NN that have a good performance to emulate the WBMOD outputs. In the case of the most complex NN, the one for the  $C_k L$ , the error achieved is under 2% from the WBMOD expected value in almost all situations, only diverging for very high solar activity values above 140 in the smoothed sun-spots number (R12). The performance of the overall fitting characterized by the mean root-squared error is  $(0.018 \pm 0.0025)\%$ .

This work opens the opportunity of using these NN to get quicker and freely available results of the scintillation parameters in all regions and all possible scenarios in terms of local time, solar, and geomagnetic activity.

## 5. REFERENCES

- [1] R. M. Bussey J. A. Secan, “An Improved Model of High-Latitude F-Region Scintillation (WBMOD version 13),” Northwest Research Associates, Inc., 1994.
- [2] J. A. Secan, R. M. Bussey, E. J. Fremouw, and Sa Basu, “High-latitude upgrade to the Wideband ionospheric scintillation model,” *Radio Science*, vol. 32, no. 4, pp. 1567–1574, 1997.
- [3] C. L. Rino, “A power law phase screen model for ionospheric scintillation: 1. Weak scatter,” *Radio Science*, vol. 14, no. 6, pp. 1135–1145, 1979.
- [4] J. Lemorton, V. Fabbro, A. Mainvis, G. González, J. Sanz, J. M. Juan, C. Molina, A. Camps, and J. Barbosa, “SCIONAV. radio climatology models of the ionosphere: Status and way forward,” techreport, European Space Agency (ESA), June 2020, Joël Lemorton and Vincent Fabbro and Aymeric Mainvis and Guillermo González and Jaume Sanz and José Miguel Juan and Carlos Molina and Adriano Camps and José Barbosa.
- [5] Adriano Camps, Carlos Molina, Guillermo González-Casado, José Miguel Juan, Joël Lemorton, Vincent Fabbro, Aymeric Mainvis, José Barbosa, and Raúl Orús-Pérez, “Ionospheric scintillation models: An inter-comparison study using GNSS data,” in *Ionosphere - New Perspectives*, Dr. Yann-Henri H. Chemin, Ed., chapter 6. IntechOpen, Rijeka, Feb 2023.
- [6] E. J. Fremouw and J. A. Secan, “Modeling and scientific application of scintillation results,” *Radio Science*, vol. 19, no. 3, pp. 687–694, 1984.